

ChemComm

Accepted Manuscript



This is an *Accepted Manuscript*, which has been through the Royal Society of Chemistry peer review process and has been accepted for publication.

Accepted Manuscripts are published online shortly after acceptance, before technical editing, formatting and proof reading. Using this free service, authors can make their results available to the community, in citable form, before we publish the edited article. We will replace this *Accepted Manuscript* with the edited and formatted *Advance Article* as soon as it is available.

You can find more information about *Accepted Manuscripts* in the [Information for Authors](#).

Please note that technical editing may introduce minor changes to the text and/or graphics, which may alter content. The journal's standard [Terms & Conditions](#) and the [Ethical guidelines](#) still apply. In no event shall the Royal Society of Chemistry be held responsible for any errors or omissions in this *Accepted Manuscript* or any consequences arising from the use of any information it contains.

COMMUNICATION

Organohalide Lead Perovskite Based Photodetectors with Much Enhanced Performance

Cite this: DOI: 10.1039/x0xx00000x

Hua-Rong Xia,^{a,b} Jia Li,^{a,c} Wen-Tao Sun^{a,b*} and Lian-Mao Peng^{a,b,c*}

Received 00th January 2012,

Accepted 00th January 2012

DOI: 10.1039/x0xx00000x

www.rsc.org/

CH₃NH₃PbI₃ based photodetectors were fabricated by a facile low-cost process with much enhanced performance. The rise time changed from 2.7s to 0.02s, the decay time from 0.5s to 0.02s, the ON/OFF ratio tripled with improved stability. The results indicate that perovskites are promising light-harvesting materials for photodetectors.

Organic-inorganic perovskites such as CH₃NH₃PbX₃ (X=Cl, Br, I) have attracted much attention as light-harvesting materials for mesoscopic solar cells with enhanced performance¹⁻⁷, since the pioneering work by Tsutomu Miyasaka et al.⁸. Photodetectors have important applications in many fields and light-harvesting material is the key part of it. However, little work has been done on the research of perovskite based photodetectors. In this work, CH₃NH₃PbI₃/TiO₂ photodetectors were fabricated by a facile and low-cost process. Compared with the plain TiO₂ photodetector, the performance was significantly improved. The response speed is much faster with the rise time of the time response constants changed from 2.7 s to 0.02 s and the decay time from 0.5 s to 0.02s. At the same time, the ON/OFF ratio is about three times of that without tCH₃NH₃PbI₃, and the stability of the photodetector was also improved. The results indicate that perovskites are promising light-harvesting materials for photodetectors.

Organohalide lead perovskite (CH₃NH₃PbI₃) was prepared according to the procedure reported by Kim et al.⁹ (Details in SI, Supporting Information). And TiO₂ paste was made from P25 powder (TiO₂ nanoparticles with diameter of about 20 nm) with a procedure similar with the report of Gratzel's group¹⁰. In a typical process, the fabrication of perovskite based photodetectors includes three steps as shown in Figure 1. First, the electrodes for photodetectors were made as the following process: the FTO area used as electrodes were protected by tapes with others exposed, then the tape-protected FTO was coated with a layer of Zinc powder and immersed into 1 M hydrochloride solution to etch the FTO without tape protection (Details in SI). Second, TiO₂ paste was coated onto the etched area to

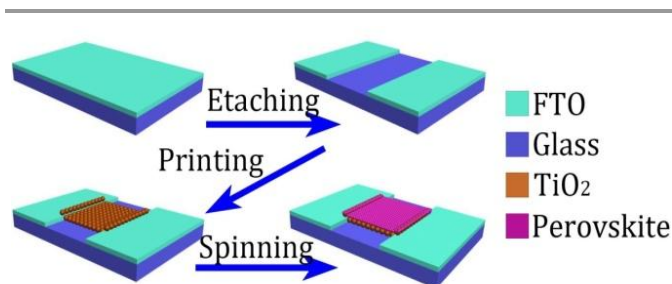


Figure 1. Scheme of the fabrication of organic-inorganic perovskite based photodetectors

link the two electrodes by a screen printing process and then annealed at 400 °C for 1 hour to form a mesoscopic film with a thickness of about 2 μm. By this way, a TiO₂-based photodetector was made indeed. Finally, the as-synthesized CH₃NH₃PbI₃ solution was spun onto the TiO₂ mesoscopic thin film and then dried at 115 °C for 15 min. Thus perovskite based photodetectors were successfully made. The performance of the photodetectors was measured by a CHI 660C electrochemical workstation under a solar simulator with AM 1.5 light. SEM (scanning electron microscope), XRD (X-ray diffraction spectrometer) and UV-Vis (ultraviolet-visible spectrometer) were also used to characterize the morphologies, structures and absorptions respectively.

The morphologies of the photodetectors were characterized by SEM with typical images shown in Figure 2a-c. Figure 2a shows an image of the conducting side of FTO glass, which is composed of large numbers of close-packed particles with the diameters from 10 to 100nm. Seen from Figure 2b, the mesoscopic TiO₂ thin film is made up of many interconnected TiO₂ nanoparticles with the diameter of about 20 nm. As there are lots of nanopores in the mesoscopic TiO₂ film, the organohalide lead perovskite solution can penetrate into them and form perovskite/TiO₂ heterojunctions. Figure 2c shows the images of CH₃NH₃PbI₃/TiO₂ film, with many perovskite penetrated into the film and others forming large flakes onto the film which is similar with the

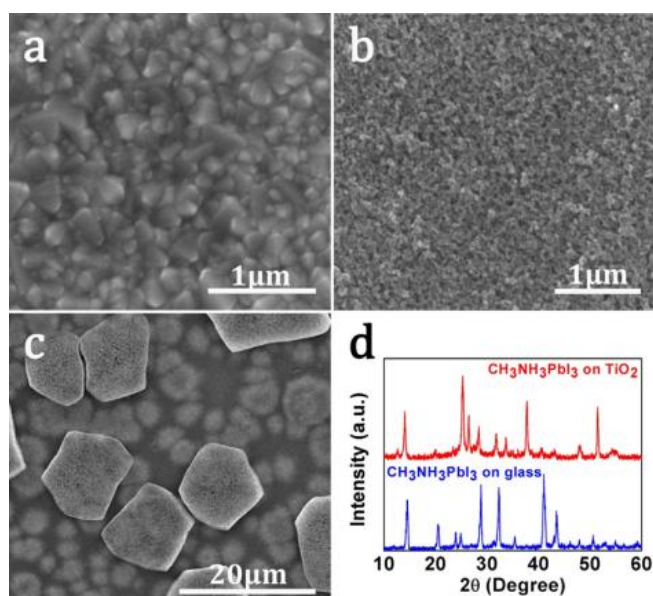


Figure 1. (a-c) SEM images of FTO glass, TiO₂ mesoscopic thin film, and CH₃NH₃PbI₃/TiO₂ thin film respectively. (d) XRD patterns of CH₃NH₃PbI₃/TiO₂ film (red line) and pure CH₃NH₃PbI₃ on a glass substrate (blue line).

reference⁴. The XRD patterns of 19.94, 28.42, 31.78, 40.48 and 43.04° are corresponding to the reflections from (110), (112), (220), (310), (224) and (314) crystal planes respectively, indicating a tetragonal perovskite structure with $a=8.855$ Å and $c=12.659$ Å (Figure 3a)¹¹. No impurity peaks other than the ones attributed to CH₃NH₃PbI₃ and TiO₂/FTO are observed, suggesting that CH₃NH₃PbI₃ grown on the mesoporous TiO₂ thin film is phase pure.

Typical transmission spectra of the etched FTO glass (black line), TiO₂ on etched FTO glass (red line) and CH₃NH₃PbI₃/TiO₂ on etched FTO glass (blue line) are shown in Figure 3b, with the corresponding photographs inset. The sharp absorption edge of the TiO₂-coated etched FTO glass has a red shift compared to that of the etched FTO glass, which may result from the smaller band gap of TiO₂ (3.2 eV) compared to SnO₂ (3.6 eV). And the significant enhanced absorption of CH₃NH₃PbI₃/TiO₂ mesoscopic thin film is ascribed to the large absorption coefficient of CH₃NH₃PbI₃⁶. Typical I-V curves of the TiO₂ photodetector and CH₃NH₃PbI₃/TiO₂ photodetector are shown in Figure 3c and 3d respectively. Clearly, I-V curves present linear dependence with the applied bias, indicating the formation of ohmic contact between TiO₂ and FTO electrode, which is crucial to photoconductive photodetectors. The dark currents at 3 V of the TiO₂ photodetector (1.34E-10 A) and the CH₃NH₃PbI₃/TiO₂ photodetector (1.36E-10 A) are similar, while the photocurrent at 3 V of the CH₃NH₃PbI₃/TiO₂ photodetector (9.75 E -9 A, corresponding responsivity 0.49 μA/W) is much larger than that of TiO₂ photodetector (3.27 E -9 A, corresponding responsivity 0.16 μA/W) showing that the introduction of CH₃NH₃PbI₃ into the TiO₂ mesoscopic photodetector improved the ON/OFF ratio (or gain) for about three times. The improvement can be attributed to the much enhanced light harvesting capability resulting from the addition of CH₃NH₃PbI₃ (shown in Figure 3b). The corresponding photocurrent time response were measured at 3V bias under a solar simulator ON/OFF switching irradiation with the light intensity of 100 mW/cm² and an ON/OFF

internal of 20 s. Ten cycle curves under ON/OFF illumination are shown in Figure 3e. It can

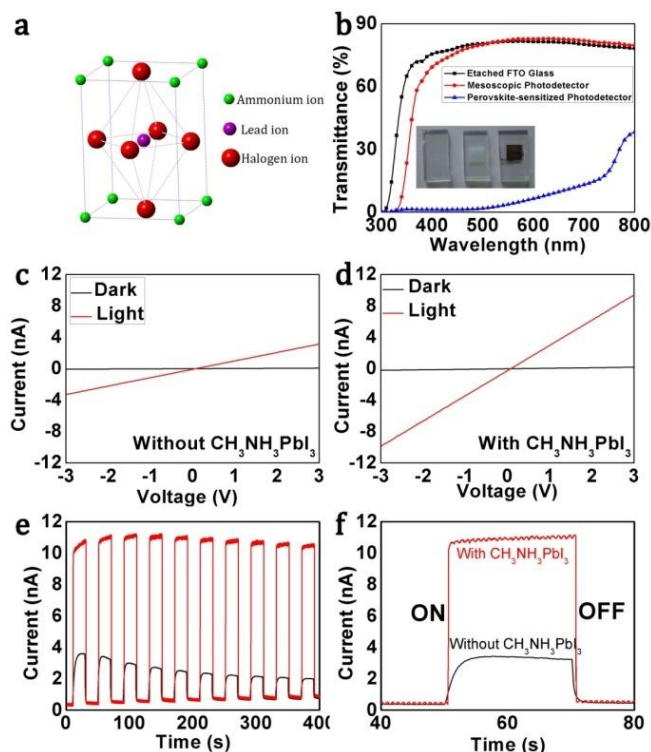


Figure 2. (a) Crystal structures of organohalide lead perovskite compounds. (b) Transmission spectra of etched FTO (black line), mesoscopic TiO₂ thin film (red line) and CH₃NH₃PbI₃/TiO₂ thin film (blue line) with the corresponding photographs inset. (c)(d) I-V curves of the photodetectors without/with CH₃NH₃PbI₃. (e)(f) Time response behaviors of the photodetectors with (red line)/without (black line) CH₃NH₃PbI₃.

be seen that the photocurrent of CH₃NH₃PbI₃/TiO₂ photodetector (red line) is consistent and repeatable while that of TiO₂ photodetector (black line) decays significantly, which is consistent with the report¹². An enlarged typical ON/OFF cycle is shown in Figure 3f, from which it can be seen that the CH₃NH₃PbI₃/TiO₂ photodetector switches much faster. To quantitatively extract the time response constant, the well accepted quantitative criterion is introduced. That is, the rise time is the time to reach 90% of the stable photocurrent, and the decay time is the time to reach 1/e (37%) of the original photocurrent¹³. According to this criterion, the rise time and decay time of the TiO₂ photodetector are about 2.7 s and 0.5 s respectively, which is comparable with the best performance of TiO₂ photodetectors reported elsewhere^{14, 15}. While the rise time and decay time of the CH₃NH₃PbI₃/TiO₂ photodetector are about 0.02 s and 0.02 s respectively.

The mechanism of the significantly shorten rise and decay time of the CH₃NH₃PbI₃/TiO₂ based photodetectors compared with the TiO₂ based ones may be described as follows. For a pure TiO₂ photodetector, it is generally accepted that the oxygen adsorption/desorption at the TiO₂ surface plays an important role and the photoresponse rate is mainly determined by the rate of oxygen adsorption/desorption.¹⁶⁻¹⁸ For a perovskite/TiO₂ heterojunction photodetector, band-bending at the interface makes it fast for the

separation of electron-hole pairs. Upon illumination, large numbers of electrons are injected into TiO₂ rapidly which increase the photoconductivity of the TiO₂ film. While when the light is switched off, the sudden absence of electron injection results in the decrease of the conductivity rapidly. Since the light-induced carrier concentration modulation is much faster than the one controlled by the oxygen adsorption/desorption process, the time response speed of the perovskite/TiO₂ photodetector is much faster than that of pure TiO₂ photodetector (Figure 5f). Besides, as the oxygen adsorption/desorption process is susceptible to the atmosphere, the cycle stability of perovskite/TiO₂ photodetector is better than that of pure TiO₂ photodetector (Figure 5e).

Conclusions

In conclusion, CH₃NH₃PbI₃/TiO₂ photodetectors were accomplished by a facile and low-cost all-solution method. The as-prepared organohalide lead perovskite (CH₃NH₃PbI₃) based photodetector has significantly enhanced performance on the time response constants and the ON/OFF ratio. The rise time changes from 2.7 s to 0.02 s and the decay time from 0.5 s to 0.02s. At the same time, the ON/OFF ratio is about three times of that without CH₃NH₃PbI₃. ON/OFF cycle experiments also indicate that the photocurrent of CH₃NH₃PbI₃/TiO₂ photodetector is more consistent and repeatable than that of plain TiO₂ photodetector. The results suggest that perovskite materials may have a promising application in photodetectors.

Acknowledgements

This work was supported by the Ministry of Science and Technology (Grant No. 2011CB933002 and 2012CB932702) and the National Science Foundation of China (Grant No. 61306079, 61171023).

Notes and references

^aKey Laboratory for the Physics and Chemistry of Nanodevices, Peking University, Beijing 100871, China

^bDepartment of Electronics, Peking University, Beijing 100871, China

^cAcademy for Advanced Interdisciplinary Studies, Peking University, Beijing 100871, China

*Email: wtaosun@pku.edu.cn; mpeng@pku.edu.cn.

† Electronic Supplementary Information (ESI) available: Experimental details of CH₃NH₃PbI₃ synthesis, preparation of TiO₂ paste, and fabrication of FTO electrodes on glass, Photographs of the CH₃NH₃PbI₃ solution, TiO₂ paste and FTO electrodes. See DOI: 10.1039/c000000x/

- M. M. Lee, J. Teuscher, T. Miyasaka, T. N. Murakami and H. J. Snaith, *Science*, 2012, **338**, 643.
- J. Burschka, N. Pellet, S.-J. Moon, R. Humphry-Baker, P. Gao, M. K. Nazeeruddin and M. Gratzel, *Nature*, 2013, **499**, 316.
- H.-S. Kim, I. Mora-Sero, V. Gonzalez-Pedro, F. Fabregat-Santiago, E. J. Juarez-Perez, N.-G. Park and J. Bisquert, *Nat Commun*, 2013, **4**, 2242.
- M. Liu, M. B. Johnston and H. J. Snaith, *Nature*, 2013, **501**, 395.
- S. D. Stranks, G. E. Eperon, G. Grancini, C. Menelaou, M. J. P. Alcocer, T. Leijtens, L. M. Herz, A. Petrozza and H. J. Snaith, *Science*, 2013, **342**, 341.
- G. Xing, N. Mathews, S. Sun, S. S. Lim, Y. M. Lam, M. Grätzel, S. Mhaisalkar and T. C. Sum, *Science*, 2013, **342**, 344.
- V. Gonzalez-Pedro, E. J. Juarez-Perez, W.-S. Arsyad, E. M. Barea, F. Fabregat-Santiago, I. Mora-Sero and J. Bisquert, *Nano Letters*, 2014, **14**, 888.
- A. Kojima, K. Teshima, Y. Shirai and T. Miyasaka, *Journal of the American Chemical Society*, 2009, **131**, 6050.
- H. S. Kim, C. R. Lee, J. H. Im, K. B. Lee, T. Moehl, A. Marchioro, S. J. Moon, R. Humphry-Baker, J. H. Yum, J. E. Moser, M. Gratzel and N. G. Park, *Scientific Reports*, 2012, **2**, 591.
- S. Ito, P. Chen, P. Comte, M. K. Nazeeruddin, P. Liska, P. Pechy and M. Gratzel, *Progress in Photovoltaics*, 2007, **15**, 603.
- Y. Zhao and K. Zhu, *The Journal of Physical Chemistry Letters*, 2013, **4**, 2880.
- G. H. Liu, N. Hoivik and K. Y. Wang, *Electrochemistry Communications*, 2013, **28**, 107.
- Y. R. Xie, L. Wei, Q. H. Li, G. D. Wei, D. Wang, Y. X. Chen, J. Jiao, S. S. Yan, G. L. Liu and L. M. Mei, *Applied Physics Letters*, 2013, **103**, 261109.
- C. H. Feng, H. F. Zhang, Y. Wang, W. Li, J. R. Zhou, L. H. Chen, L. X. Yu and S. P. Ruan, *Journal of the American Ceramic Society*, 2012, **95**, 1980.
- J. Zou, Q. Zhang, K. Huang and N. Marzari, *The Journal of Physical Chemistry C*, 2010, **114**, 10725.
- S. Zhang, C. Xie, Z. Zou, L. Yang, H. Li and S. Zhang, *The Journal of Physical Chemistry C*, 2012, **116**, 19673.
- W. Zhang, J.-K. Huang, C.-H. Chen, Y.-H. Chang, Y.-J. Cheng and L.-J. Li, *Advanced Materials*, 2013, **25**, 3456.
- G. H. Liu, N. Hoivik, X. M. Wang, S. S. Lu, K. Y. Wang and H. Jakobsen, *Electrochimica Acta*, 2013, **93**, 80-86.